Introduction

The boundary layers that form on hypersonic cruise vehicles are turbulent and chemically reacting. The chemical reactions alter the temperature distribution on the boundary layer, modifying the heating rates. To aid the design of these vehicles, an accurate prediction of the chemical composition of the gas is needed.

$k-\epsilon$ turbulence models are widely used to simulate hypersonic flows. These models predict high speed perfect gas flows accurately. However, there are some model uncertainties when simulating chemically reacting flows. With the very high energies present in these flows, the temperature fluctuations will be very large. The reaction rate depends exponentially on temperature, and temperature fluctuations result in large increases in the reaction rates. Also, the chemical source term can either damp or amplify turbulent fluctuations; this effect has been seen experimentally by several researchers. Johnson *et al.*[-] have also shown that hypersonic boundary layers tend to be stabilized by endothermic reactions and destabilized by exothermic reactions.

It is illustrative to consider the $k-\epsilon$ and direct numerical simulation (DNS) results for a non-reacting turbulent boundary layer at Mach 4 and $Re_\theta = 800$. Figure 1 plots the mean temperature given by the $k-\epsilon$ model of Jones and Launder. In this case, the temperature is high enough to induce chemical reactions. Figure 2 plots the magnitude of the temperature fluctuations for the same case obtained from the DNS of Martín *et al.*[-] We observe that the maximum temperature fluctuations are nearly 15% of the mean temperature. Therefore, to obtain accurate reaction rates, the temperature fluctuations must be modeled.

A general method for the closure of a non-linear chemical source term in the RANS approach is to use a probability density function (PDF)[-] in which the unclosed species production term is represented by a PDF in terms of the independent variables. The PDF can be computed using a modeled balance equation for the same or using a Monte-Carlo method.[,] These tend to be computationally expensive for practical problems. An alternative approach is to assume a generic shape and compute only the parameters that define the PDF. This reduces the computational cost considerably. Following this latter approach, Gaffney *et al.* assume a shape for the temperature fluctuation PDF and investigate how the fluctuations affect the combustion process. They need two parameters to obtain the PDF, the mean and the standard deviation. The mean is obtained from the solution of the Favre-averaged Navier-Stokes equations and the standard deviation is calculated by solving an extra transport equation for the energy variance. Martín and Candler[-] used a similar approach to model the temperature fluctuations in reacting, isotropic turbulence. In particular, a shape of the PDF is assumed based on DNS data and the parameters that describe the PDF are computed using calibrated mean turbulence values.

In the Gaffney *et al.* model, a transport equation is derived for the energy variance and then the unclosed higher moments in the equation are modeled in terms of the average quantities. This model and similar ones' have been applied to flow problems where the predictions of the average flow quantities are compared with their experimental values. This assesses the overall performance of the model but does not evaluate the assumptions made for each unclosed term. In this regard, a DNS database is very useful wherein the unclosed terms can be computed exactly and compared to their modeled counterpart. This is the approach that will be taken in this work to evaluate the model. Similarly, the Martín and Candler model will also be assessed.

In the next section, these turbulence-chemistry models are delineated along with a brief description of the $k-\epsilon$ approach. This is followed by the comparison of these models to the DNS of homogeneous isotropic turbulence. The conclusions are presented at the end.

Numerical Method

In case of homogeneous isotropic turbulence, the gradients of the mean flow quantities are zero. Thus there is no mean convection or diffusion. As a result, the mean density, $\bar{\rho}$, the mean velocity components, $\tilde{u}_i$ and the mean total energy, $\tilde{E}$, remain constant in the flow. In these simulations,

$$\begin{aligned} \bar{\rho} &= 0.5 \quad \text{kg/m}^3 \\ \tilde{u}_i &= 0 \quad \text{for i=1,2,3} \\ \tilde{E} &= \bar{\rho}\bar{c}_v\tilde{T} + \tfrac{1}{2}\bar{\rho}\tilde{u}_i\tilde{u}_i + \bar{\rho}k + \sum_s \bar{\rho}_s h_s^0. \end{aligned} \tag{1}$$

The over-bar represents Reynolds averaging whereas the tilde represents the Favre-averaged quantities. $\bar{c}_v$ is the average specific heat of the mixture at constant volume, $\tilde{T}$ is the average temperature, $\bar{\rho}_s$ and h_s^0 are the density and heat of formation of species s in the mixture, and k is the turbulent kinetic energy given by

$$\bar{\rho}k = \tfrac{1}{2}\overline{\rho u_i'' u_i''}$$

Here we study the reversible bimolecular dissociation of N_2 in a two species mixture.

$$\mathrm{N_2 + M \rightleftharpoons 2N + M\ .} \tag{2}$$

The conservation of N_2 is given by

$$\frac{\partial \bar{\rho}_1}{\partial t} = \bar{w}_1 \tag{3}$$

where w_1 represents the rate of production or consumption of N_2 due to the reversible dissociation reaction and is given by

$$w_1 = -M_1 k_f \left(\frac{\rho_1}{M_1}\right)\left(\frac{\rho_1}{M_1}+\frac{\rho_2}{M_2}\right) + M_1 k_b \left(\frac{\rho_2}{M_2}\right)^2 \left(\frac{\rho_1}{M_1}+\frac{\rho_2}{M_2}\right) \tag{4}$$

where M_1 and M_2 are the molecular masses of N_2 and N, respectively. k_f and k_b are the forward and backward rate constants and are given by

$$\begin{aligned} k_f &= CT^{\eta} e^{-\theta/T} \\ k_b &= k_f / K_{eq} \end{aligned} \tag{5}$$

where C, η and θ are experimentally determined constants, and K_{eq} is the known temperature-dependent equilibrium constant. Thus the reaction rate, w_1, depends on the species concentrations and the temperature via the rate constants. In hypersonic flows, the reactions are mostly temperature limited and therefore the effect of the fluctuations in the species concentrations is neglected while computing the mean reaction rate, $\bar{w}_1$. However, the effect of the temperature fluctuations is accounted for using a Probability Distribution Function, $P(T)$.

$$\bar{w}_1 = -M_1 \bar{k}_f \left(\frac{\bar{\rho}_1}{M_1}\right)\left(\frac{\bar{\rho}_1}{M_1}+\frac{\bar{\rho}_2}{M_2}\right) + M_1 \bar{k}_b \left(\frac{\bar{\rho}_2}{M_2}\right)^2 \left(\frac{\bar{\rho}_1}{M_1}+\frac{\bar{\rho}_2}{M_2}\right) \tag{6}$$

where

$$\begin{aligned} \bar{k}_f &= \int_0^\infty k_f(T) P(T) dT \\ \bar{k}_b &= \int_0^\infty k_b(T) P(T) dT. \end{aligned} \tag{7}$$

DNS of these flows have found the Probability Distribution Function to be Gaussian,

$$P(T) = \frac{1}{\sqrt{2\pi \widetilde{T''T''}}} \exp\left[\frac{-(T-\tilde{T})^2}{2\widetilde{T''T''}}\right], \tag{8}$$

where $\widetilde{T''T''}$ is the temperature variance and is evaluated using turbulence-chemistry models discussed later in this section.

The exact governing equation for k in homogeneous turbulence is given by

$$\bar{\rho}\frac{\partial k}{\partial t} = -\overline{t_{ij} u''_{i,j}} + \overline{p' u''_{i,i}} = -\bar{\rho}\epsilon_s - \bar{\rho}\epsilon_c + \overline{p' u''_{i,i}} \tag{9}$$

where t_{ij} is the viscous stress tensor and p' is the pressure fluctuation. ϵ_s and ϵ_c are the solenoidal and compressible part of dissipation, respectively, and are given by

$$\begin{aligned} \bar{\rho}\epsilon_s &= \bar{\nu}\overline{\rho \omega''_i \omega''_i} \\ \bar{\rho}\epsilon_c &= \bar{\nu}\overline{\tfrac{4}{3}\rho u''_{i,i} u''_{j,j}} \end{aligned}$$

The compressible dissipation and the pressure dilatation terms are modeled in terms of the solenoidal dissipation.

$$\begin{aligned} \bar{\rho}\epsilon_c &= \bar{\rho}\epsilon_s(\alpha_1 M_t^2) \\ \overline{p' u''_{i,i}} &= \bar{\rho}\epsilon_s(\alpha_3 M_t^2) \end{aligned} \tag{10}$$

where $\alpha_1 = 1$, $\alpha_3 = 0.2$ and M_t is the turbulent Mach number given by

$$M_t^2 = \frac{2k}{\gamma R \tilde{T}}$$

The exact governing equation for ϵ_s in homogeneous turbulence is given by

$$\begin{aligned} \frac{\partial}{\partial t}(\bar{\nu}\overline{\rho\omega''_i\omega''_i}) = & \underbrace{-\bar{\nu}\,\overline{u''_j \frac{\partial}{\partial x_j}(\rho\omega''_i\omega''_i)}}_{D_{\epsilon 1}} \underbrace{-3\bar{\nu}\overline{\rho\omega''_i\omega''_i u''_{j,j}}}_{D_{\epsilon 2}} - \underbrace{2\bar{\nu}^2\rho\overline{\frac{\partial\omega''_i}{\partial x_j}\frac{\partial\omega''_i}{\partial x_j}}}_{\Phi_\epsilon} \\ & + \underbrace{2\bar{\nu}\overline{\rho\omega''_i\omega''_j u''_{i,j}}}_{P_\epsilon} + \underbrace{2\bar{\nu}\frac{e_{ijk}}{\bar{\rho}^2}\overline{\rho\omega''_i\rho'_{,j}p'_{,k}}}_{B_\epsilon} \end{aligned} \tag{11}$$

The first two terms on the right hand side represent diffusion of ϵ_s due to turbulent mixing and the third term is the turbulent dissipation of ϵ_s. The last two terms represent production of solenoidal dissipation due to turbulence and due to baroclinic torques. The turbulent diffusion terms are modeled using the gradient diffusion assumption. They are expected to be negligible in a homogeneous turbulent flow because of the absence of mean gradients. As pointed out by Mansour *et al.*, the turbulent production term and the dissipation term are together modeled as

$$+2\bar{\nu}\overline{\rho\omega''_i\omega''_j u''_{i,j}} - 2\bar{\nu}^2\rho\overline{\frac{\partial\omega''_i}{\partial x_j}\frac{\partial\omega''_i}{\partial x_j}} \quad \sim \quad -c_2\frac{\bar{\rho}\epsilon^2}{k} \tag{12}$$

Gaffney *et al.* model

The temperature variance, $\widetilde{T''T''}$, is obtained from the energy variance, $\widetilde{e''e''}$. Here, e is the internal energy of the mixture, $e = c_v T + \sum c_s h_s^0$. In homogeneous turbulence, the transport equation for the energy variance has the following form,

$$\begin{aligned} \frac{\partial\bar{\rho}\tilde{g}}{\partial t} &= 2\,\overline{e''\left(\tau_{ij}\frac{\partial u_i}{\partial x_j} - \frac{\partial q_j}{\partial x_j} - p\frac{\partial u_j}{\partial x_j} + \frac{\partial}{\partial x_j}\rho\mathcal{D}\sum_s h_s\frac{\partial c_s}{\partial x_j}\right)} \\ &= 2\left[\underbrace{\overline{e''\tau_{ij}\frac{\partial u_i}{\partial x_j}}}_{S1} + \underbrace{\overline{e''\frac{\partial}{\partial x_j}\kappa\frac{\partial T}{\partial x_j}}}_{S2} - \underbrace{\overline{e''p\frac{\partial u_j}{\partial x_j}}}_{S3} + \underbrace{\overline{e''\frac{\partial}{\partial x_j}\rho\mathcal{D}\sum_s h_s\frac{\partial c_s}{\partial x_j}}}_{S4}\right], \end{aligned} \tag{13}$$

where $g = e''e''$, τ_{ij} is the viscous stress tensor and q_j is the heat flux vector defined in terms of the conductivity, κ, and the gradient of temperature. h_s and c_s are the specific enthalpy and mass fraction, respectively, of species s and $\mathcal{D}$ is the diffusivity. The various unclosed terms are modeled and the resulting modeled equation in case of homogeneous turbulence is

$$\frac{\partial \bar{\rho}\tilde{g}}{\partial t} == -2\bar{\rho}\epsilon_g = -2C_g\bar{\rho}\tilde{g}\frac{\epsilon}{k} \ . \tag{14}$$

The temperature variance, $\widetilde{T''T''}$, is obtained as

$$\widetilde{T''T''} = \frac{\widetilde{e''e''}}{\hat{c}_v^2} \ , \tag{15}$$

where

$$\hat{c}_v = \frac{1}{T}\int_0^T c_v(T)\, dT \ .$$

More details can be found in the original reference.

Martín and Candler model

Martín and Candler study the interaction between decaying isotropic turbulence and finite-rate chemical reactions at conditions typical of a hypersonic boundary layer. Their results confirmed that the interaction is characterized by the increased or decreased magnitude of the temperature fluctuations for exothermic or endothermic reactions, respectively. They use the DNS database to develop a model for the temperature fluctuations, using a probability density representation. The DNS database revealed a physically consistent relationship between the resolved-scale flow conditions, that may be used to predict the standard deviation of the Gaussian PDF for the temperature fluctuations. Specifically, for isotropic turbulence with $\mathrm{N_2 + M \rightleftharpoons 2N + M}$ reactions (M is the collision partner),

$$\frac{\sqrt{\widetilde{T''T''}}}{\tilde{T}} = \begin{cases} A\left(\overline{\Delta h^\circ}\lambda/l_E\right)^{\mathrm{B}} & \text{if exothermic ;} \\ C M_t^2 & \text{if endothermic.} \end{cases} \tag{16}$$

where $\overline{\Delta h^o}$ is the non-dimensionalized heat release, λ is the Taylor microscale and l_E is the expansion length defined as the distance traveled by the acoustic radiation from the chemistry induced temperature fluctuations. M_t and Da are the turbulent Mach number and the Damköhler number, respectively, and A, B and C are calibrated constants. The mean temperature is, once again, obtained from the average energy conservation equation. Further details of the model can be found in Ref. 12. The model has been calibrated and tested by comparison to simulations of decaying isotropic turbulence. The single-variable PDF model was found to capture the fluctuations in temperature and product formation.

Results

As a test case, we solve a homogeneous isotropic turbulence flow field with Reynolds number based on the Taylor micro-scale, Re_λ, of 35 and an initial turbulent Mach number of 0.7 . The initial concentration of N_2 is 0.3 . The non-reacting flow is simulated until $t/\tau_t = 2$ to obtain fully developed turbulence. Here $\tau_t = \lambda/u'$ is the characteristic turbulent time-scale. The reactions are then started and time is reset to 0. All the data presented in this section is based on this reference time.

First, we check the accuracy of the $k-\epsilon$ turbulence model. To do that we compare the various terms in the transport equation for k, Eq. (9), and evaluate their modeling. Figure 3 presents the budget of the k-equation. We see that the solenoidal dissipation is the most dominant term whereas the compressible dissipation is small throughout the simulation. The pressure dilatation term is also small except for the initial peak due to the exothermic reaction. It is to be noted that the heat released in the chemical reactions increases the turbulence level in the flow via this pressure-dilatation term. The compressible dissipation is modeled in terms of the solenoidal dissipation times $\alpha_1 M_t^2$ with $\alpha_1 = 1$. Figure 4 compares the ratio of the two dissipations to the magnitude of M_t^2. It can be seen that the present simulation gives $\alpha_1 = 0.25$ instead of 1.0 as obtained by Sarkar. The amount of compressibility in a Direct Numerical Simulation of homogeneous isotropic turbulence depends on the initialization of the flow field and thus can vary in different simulations. The pressure dilatation term is modeled in terms of ϵ_s as shown in equation (10). Once again, we check the accuracy of this modeling in figure 5 by comparing the ratio $\overline{p' u''_{i,i}}/\rho\epsilon_s$ to $\alpha_3 M_t^2$. It is seen that the model captures the magnitude of the term, except for the initial peak. Also, there are oscillations in the pressure-dilatation term that are not reproduced by the model.

Next, we study the ϵ-equation. Figure 6 presents the five terms as identified in Eq. (11). We see that the dissipation term, Φ_ϵ and the turbulent production term, P_ϵ are dominant in this flow and the turbulent diffusion terms, $D_{\epsilon 1}$ and $D_{\epsilon 2}$, are comparatively small. Also the baroclinic torques have very little contribution to the overall budget. Comparison of $P_\epsilon - \Phi_\epsilon$ with its modeled counterpart $-c_2\bar{\rho}\epsilon^2/k$ in fig. 7 shows that the modeling is reasonable only after the initial transience ($t/\tau_t > 1$).

In the region after the initial transience the compressible dissipation and pressure-dilatation term in the k-equation are less than 5% of the solenoidal dissipation. Also, these terms have opposite effects on rate of change of k, namely,

$$-\bar{\rho}\epsilon_c + \overline{p' u''_{i,i}} \simeq -\bar{\rho}_s(\alpha_1 - \alpha_3)M_t^2$$

with $\alpha_1 = 0.25$ and $\alpha_3 = 0.2$. Therefore, neglecting these terms has a negligible effect on the rate decay of the turbulent kinetic energy. However, dropping the dependence on

$\tilde{T}$ in M_t decouples the $k-\epsilon$ equations from the mean flow equations and can be solved independently. This helps in differentiating the deficiencies of the $k-\epsilon$ model from those of the turbulence-chemistry models. Thus the equations to be solved are

$$\begin{aligned} \frac{\partial k}{\partial t} &= \epsilon_s \\ \frac{\partial \epsilon_s}{\partial t} &= c_2 \epsilon_s^2 / k \end{aligned} \tag{17}$$

with initial conditions k_0 and ϵ_0 at time t_0. The solution to this initial value problem is of the form

$$\begin{aligned} k &= k_0 \left(1 + \frac{t}{\tau_0}\right)^{-n} \\ \epsilon_s &= \epsilon_0 \left(1 + \frac{t}{\tau_0}\right)^{-(n+1)} \end{aligned} \tag{18}$$

where $n = 1/(c_2 - 1)$ and $\tau_0 = nk_0/\epsilon_0$. We use $c_2 = 1.8$ corresponding to Chien's model. Figure 8 and 9 compares the decay of k and ϵ as predicted by the model to that in the DNS. It can be seen that starting at $t_0/\tau_t = 1$, the turbulence model does a reasonably good job in predicting the decay.

Next, we study the chemistry modeling in terms of the species density of N_2, $\bar{\rho}_1$. The variation of $\bar{\rho}_1$ is given by the Eq. (3) where the average source term is a non-linear function of the mean flow variables and the turbulence parameters.

$$\frac{\partial \bar{\rho}_1}{\partial t} = \bar{w}_1(\tilde{T}, \bar{\rho}_1, \bar{\rho}, k, \epsilon, \widetilde{T''T''})$$

Here, $\bar{\rho}$ is constant and $\tilde{T}$ can be obtained from the conservation of total mean energy, Eq. (1). The turbulent parameters, k and ϵ are already known from solving their decoupled governing equations. Finally, the temperature variance, $\widetilde{T''T''}$, is evaluated using the turbulence chemistry models. We first study the Gaffney *et al.* model followed by the model by Martin and Candler.

As pointed out in the earlier section, in the Gaffney *et al.* model, $\widetilde{T''T''}$ is obtained from the energy variance, $\widetilde{e''e''}$, using Eq. (15). If the specific heat of the mixture is independent of temperature, as is the case in these simulations, then Eq. (15) simplifies to

$$\widetilde{T''T''} = \frac{\widetilde{e''e''}}{\bar{c}_v^2}. \tag{19}$$

This equation is arrived at by making certain assumptions which become clear when we look at all the contributions to $\widetilde{e''e''}$. In this flow case, we have a mixture of N_2, with

zero heat of formation, and N, with a heat of formation h_2^0. Thus the internal energy of the mixture can be written as

$$e = c_v T + c_2 h_2^0 = (c_1 c_{v1} + c_2 c_{v2})T + c_2 h_2^0$$

where c_1 and c_2 are the mass fractions of N_2 and N, respectively, and c_{v1} and c_{v2} are the corresponding specific heat at constant volume. Using the above form, we derive an expression for the energy variance as follows,

$$\widetilde{e''e''} = \bar{c}_v^2 \widetilde{T''T''} + \beta_1^2 \widetilde{c_1''c_1''} + \beta_2^2 \widetilde{c_2''c_2''} + 2\bar{c}_v\beta_1 \widetilde{c_1''T''} + 2\bar{c}_v\beta_2 \widetilde{c_2''T''} + 2\beta_1\beta_2 \widetilde{c_1''c_2''} \qquad (20)$$

where $\beta_1 = c_{v1}\tilde{T}$ and $\beta_2 = c_{v2}\tilde{T} + h_2^0$. The third and fourth order correlations are neglected in arriving at the above equation. Thus we see that Eq. (19) is true only if the last five terms in the above equation are negligible. We compare the magnitudes of the various contributions to $\widetilde{e''e''}$ as obtained from DNS in Fig. 10. We see that the $\widetilde{T''T''}$ term has the biggest contribution to the energy variance but the effects of the $\widetilde{c_2''c_2''}$ and the $\widetilde{c_2''T''}$ terms are not negligible. The remaining three terms are relatively small.

Next, we study the various terms in the transport equation for $\widetilde{e''e''}$, Eq. (13). The magnitude of the source terms on the right-hand side as obtained from DNS are shown in Fig. 11. The first term, $S1$, represents the dissipation of turbulent energy into the internal energy and is a source term for $\widetilde{e''e''}$. The second term accounts for the decay of internal energy fluctuations due to heat conduction. It acts as a sink of the energy variance and has a dominating effect in the transport of $\widetilde{e''e''}$. The third term is the correlation of the energy fluctuation with the pressure work. From the DNS data, we see that this term is large and oscillating. The transport equation for $\widetilde{e''e''}$ in homogeneous isotropic turbulence is modeled as Eq. (14) where the modeled term corresponds to the dissipative effect of $S2$. Comparing the magnitude of $S2$, in Fig. 12, to its modeled counterpart $-2C_g\bar{\rho}\epsilon/k$ as obtained from DNS shows that they are quite different. The term $\partial\bar{\rho}\tilde{g}/\partial t$ is also shown in the figure. It can be seen that Eq. (14) does not hold in this flow and better modeling of the transport equation is required.

Next, we use the Martin *et al.* model, Eq. (16), to evaluate $\widetilde{T''T''}$. The constants A, B and C are obtained by calibrating the DNS data, as shown in Fig. 13. The Taylor micro-scale in this homogeneous isotropic turbulence is given by

$$\lambda = \sqrt{10\,\bar{\nu}\,\frac{k}{\epsilon}}$$

Thus using the turbulence-chemistry models to evaluate $\widetilde{T''T''}$, we get a first order system for $\bar{\rho}_1$ and it is solved using fourth order Runge Kutta method with initial value of $\bar{\rho}_1$ matched at $t/\tau_t = 1$.

Figure 14 shows the variation of the rms temperature normalized by $\tilde{T}$ as obtained by DNS and the turbulence-chemistry models. Initially, the temperature fluctuations are as high as 10% of the mean and they decay as the reaction slows down. It can be seen that Martin and Candler model reproduces the temperature variance after $t/\tau_t = 1$ very well. The initial high values of the temperature fluctuations could not be reproduced because of the limitations of the $k-\epsilon$ turbulence model. On the other hand, the Gaffney *et al.* model overpredicts the temperature fluctuations mainly because of neglecting the various contributions to $\widetilde{e''e''}$ in Eq. (20). Next, we look at the forward rate constant, k_f, in Fig. 15. It is to be noted that the forward reaction is exothermic direction. It can be seen from the DNS data, that as the reaction proceeds and the temperature of the mixture rises due to dissociation of N_2, the rate of the forward reaction also increases. The Gaussian PDF with $\widetilde{T''T''}$, as obtained from Martin and Candler model, is used to evaluate the integrated value of the forward rate constant and it matches well with $\bar{k}_f$ obtained from DNS. On the other hand, k_f evaluated at the mean temperature, $\tilde{T}$, is smaller than $\bar{k}_f$. The average forward rate constant evaluated using the temperature variance from the Gaffney *et al.* model is higher than $\bar{k}_f$ from DNS and than that predicted by the Martin and Candler model. Finally, the average reaction rate, $\bar{w}_1$, and the variation of species density of N_2 are presented in Fig. 16 and 17, respectively. There is little difference between the predictions of the two models.

Conclusions

In this paper, we use Direct Numerical Simulation of homogeneous isotropic turbulence to evaluate the accuracy of turbulence-chemistry models. We use the standard $k-\epsilon$ model to simulate the turbulence field. The $k-\epsilon$ model is found to work well in this flow field except for the initial transient regime of the flow. The turbulence-chemistry model of Gaffney *et al.* solves a modeled transport equation for the internal energy variance. Comparison with the DNS shows that the modeling of the terms in the transport equation are inadequate in reproducing the observed trends. Also, correlations including species concentration fluctuations are neglected while obtaining the temperature variance from the internal energy variance. This leads to additional errors as a result of which the Gaffney *et al.*model overpredicts the temperature fluctuations in the flow. Finally, the Martin and Candler model is found to predict the temperature fluctuations as well as the average reaction rate constants accurately.

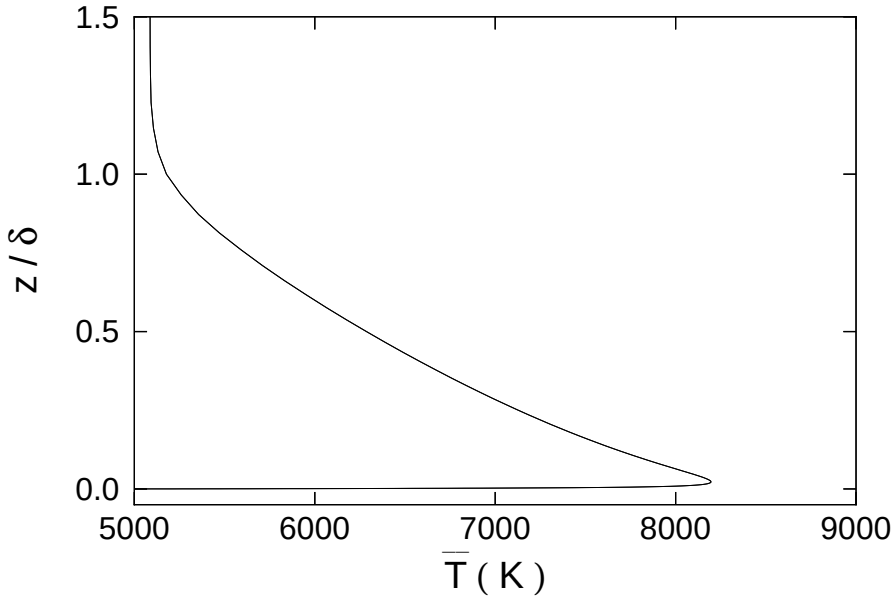

FIGURE 1. Average temperature across a turbulent boundary layer at $M = 4$ obtained using $k - \epsilon$ turbulence model.

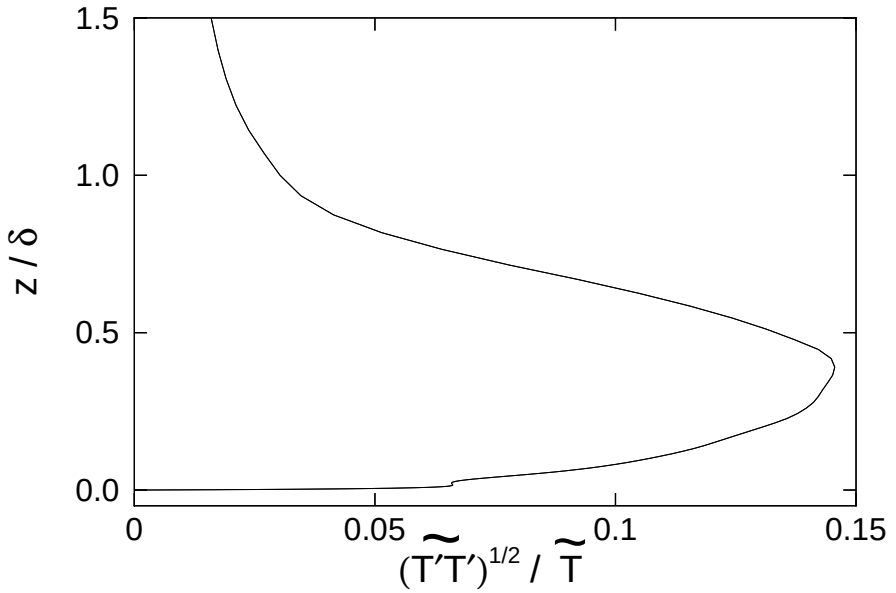

FIGURE 2. Non-dimensional temperature fluctuation magnitude for a turbulent boundary layer at $M = 4$ obtained using DNS.

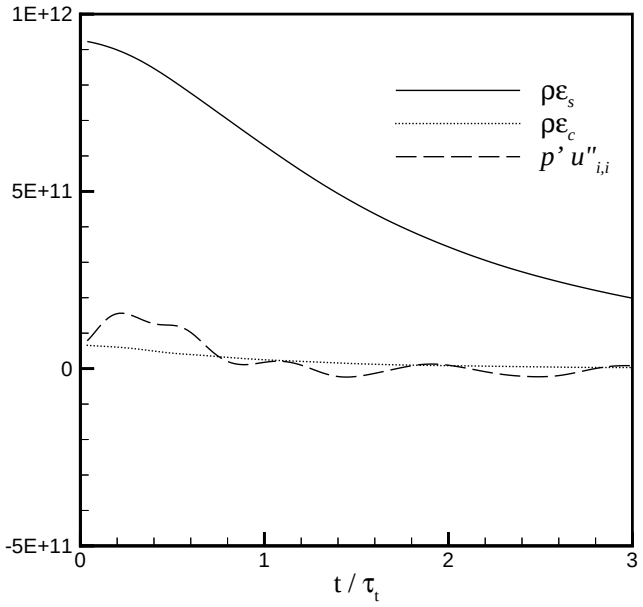

FIGURE 3. k-equation budget in a homogeneous isotropic turbulence flow field at $Re_\lambda = 35$ and initial $M_t = 0.7$.

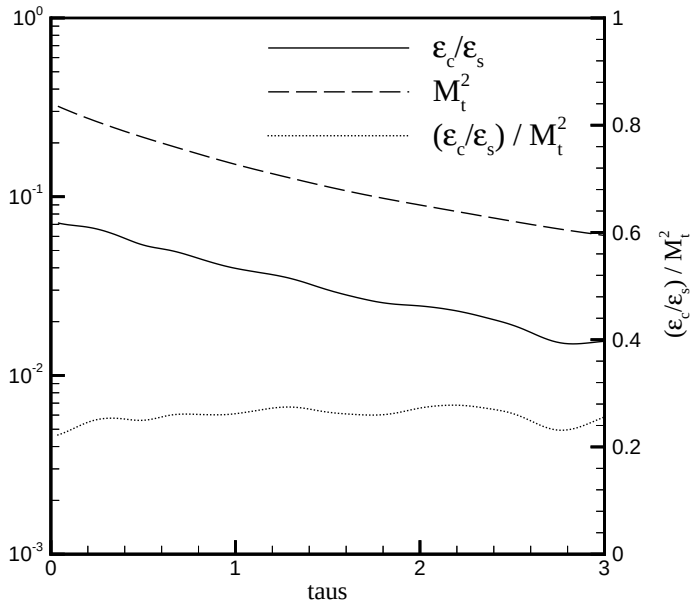

FIGURE 4. Modeling of compressible dissipation in a homogeneous isotropic turbulence flow field at $Re_\lambda = 35$ and initial $M_t = 0.7$.

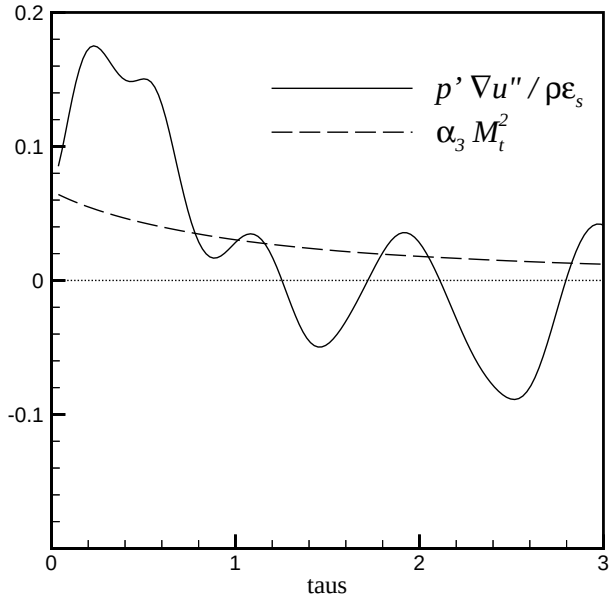

FIGURE 5. Modeling of the pressure-dilatation correlation in a homogeneous isotropic turbulence flow field at $Re_\lambda = 35$ and initial $M_t = 0.7$.

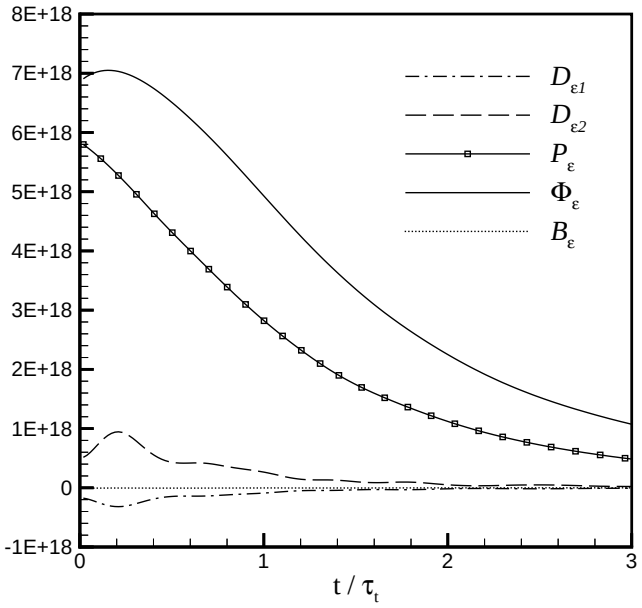

FIGURE 6. ϵ-equation budget in a homogeneous isotropic turbulence flow field at $Re_\lambda = 35$ and initial $M_t = 0.7$.

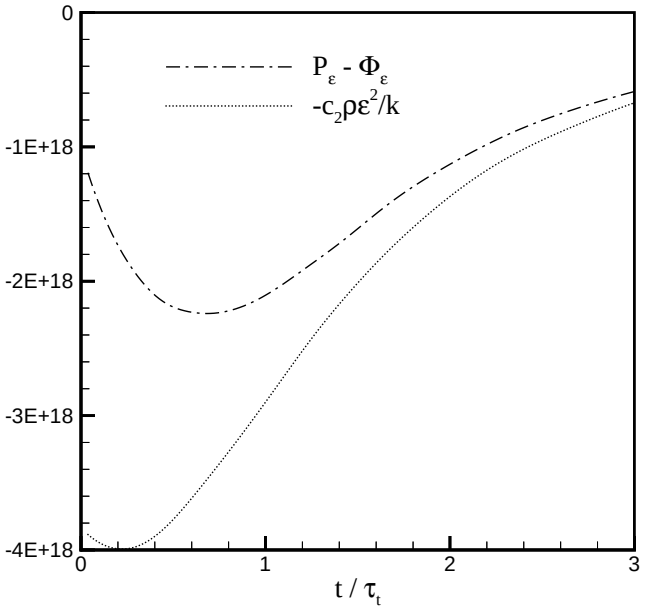

FIGURE 7. Modeling of ϵ-equation in a homogeneous isotropic turbulence flow field at $Re_\lambda = 35$ and initial $M_t = 0.7$.

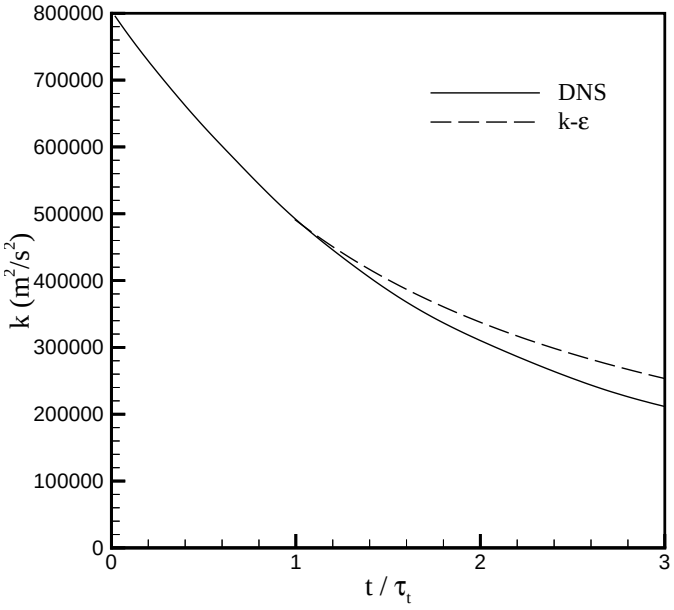

FIGURE 8. Decay of turbulent kinetic energy in a homogeneous isotropic turbulence flow field at $Re_\lambda = 35$ and initial $M_t = 0.7$.

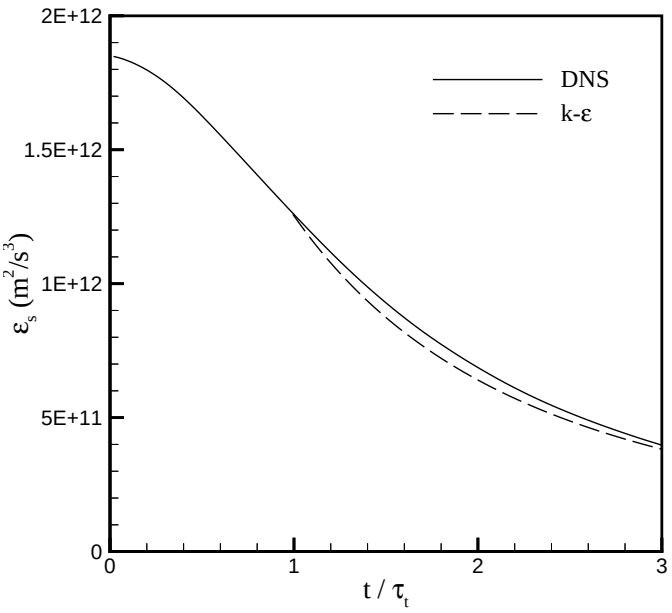

FIGURE 9. Decay of solenoidal dissipation in a homogeneous isotropic turbulence flow field at $Re_\lambda = 35$ and initial $M_t = 0.7$.

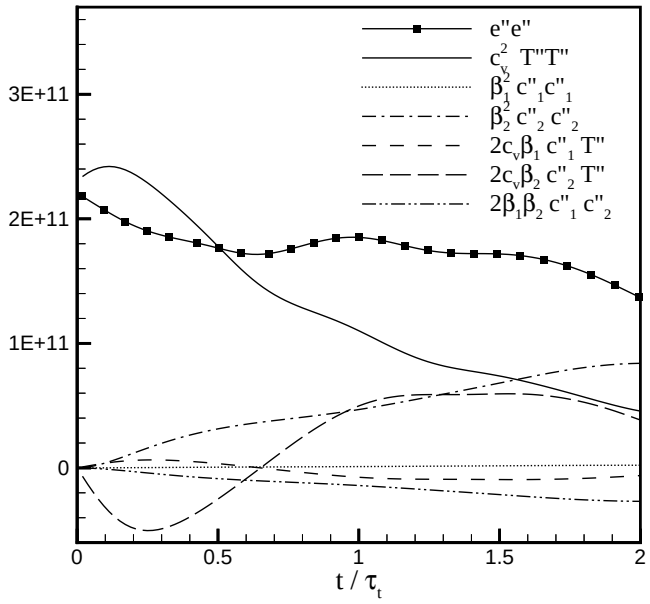

FIGURE 10. Contributions to $\widetilde{e''e''}$ in a homogeneous isotropic turbulence flow field at $Re_\lambda = 35$ and initial $M_t = 0.7$.

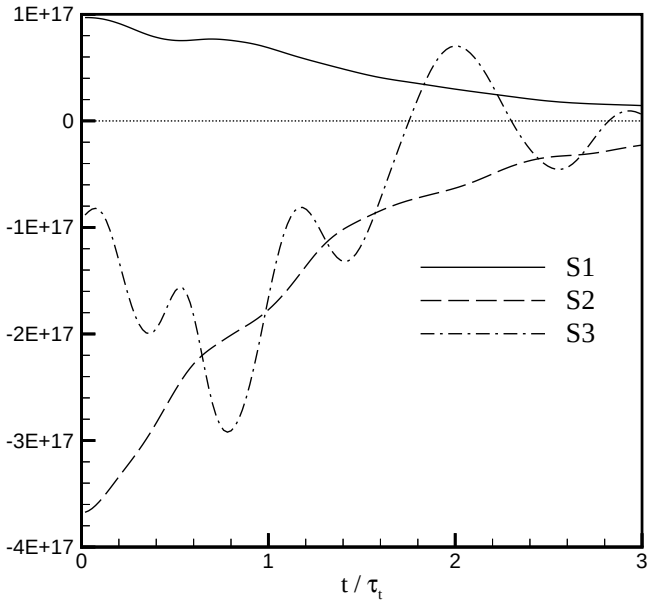

FIGURE 11. Budget of $\widetilde{e''e''}$ equation in a homogeneous isotropic turbulence flow field at $Re_\lambda = 35$ and initial $M_t = 0.7$.

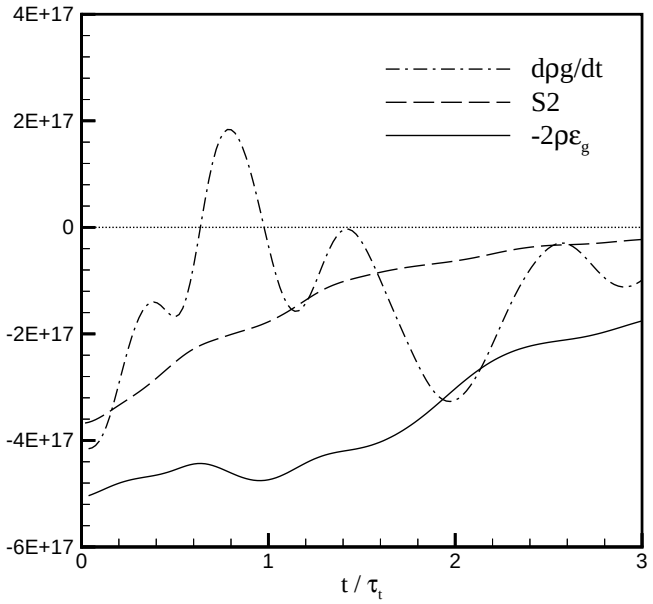

FIGURE 12. Modeling of $\widetilde{e''e''}$ equation in a homogeneous isotropic turbulence flow field at $Re_\lambda = 35$ and initial $M_t = 0.7$.

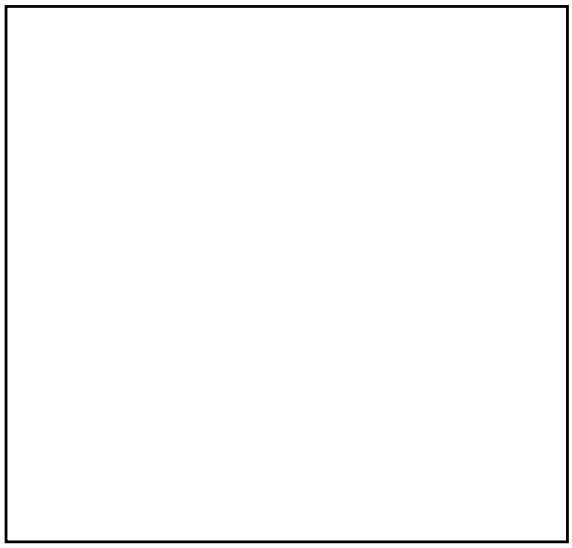

FIGURE 13. Calibration curve for Martin Model in a homogeneous isotropic turbulence flow field at $Re_\lambda = 35$ and initial $M_t = 0.7$.

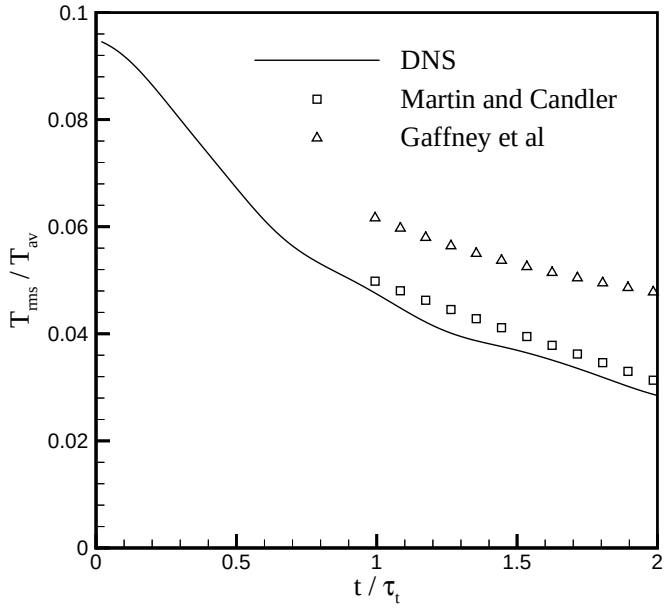

FIGURE 14.Variation of rms Temperature fluctuation in a homogeneous isotropic turbulence flow field at $Re_\lambda = 35$ and initial $M_t = 0.7$.

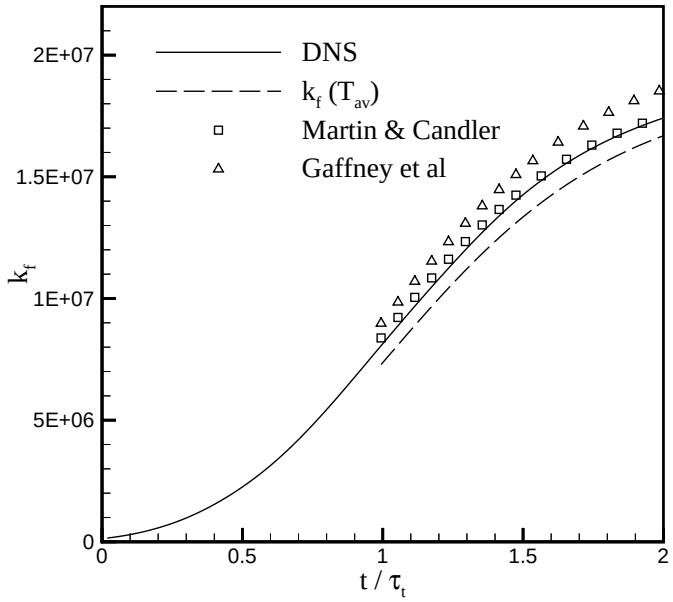

FIGURE 15.Variation of forward rate constant in a homogeneous isotropic turbulence flow field at $Re_\lambda = 35$ and initial $M_t = 0.7$.

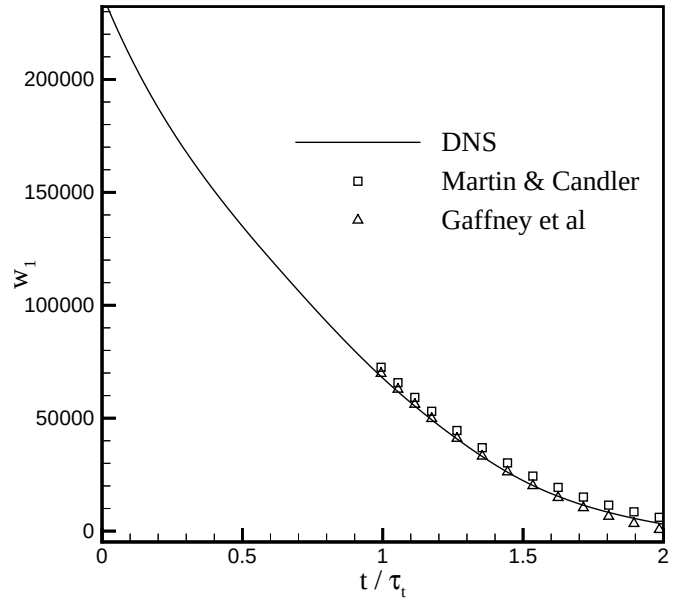

FIGURE 16.Rate of reaction in a homogeneous isotropic turbulence flow field at $Re_\lambda = 35$ and initial $M_t = 0.7$.

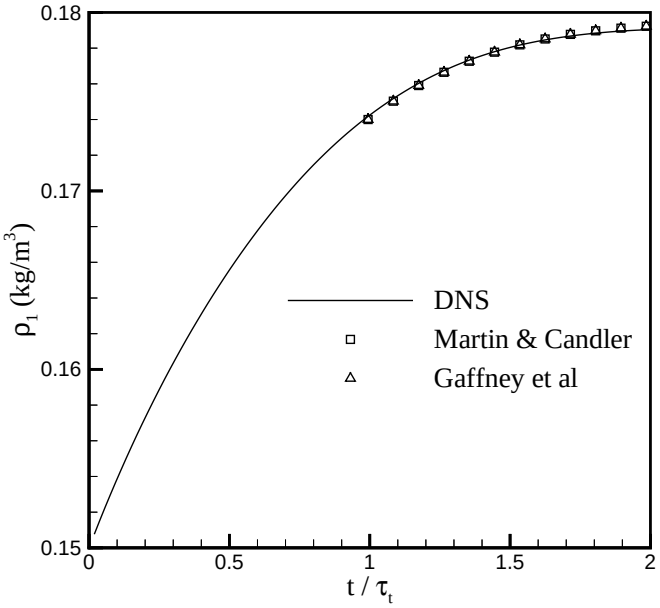

FIGURE 17.Variation of N_2 density in a homogeneous isotropic turbulence flow field at $Re_\lambda = 35$ and initial $M_t = 0.7$.